PHOTOSYNTHETICA
International Journal for Photosynthesis Research

DOI 10.32615/ps.2023.042 PHOTOSYNTHETICA 61 (SI): 473-482, 2023

Special issue in honor of Prof. Győző Garab

Monitoring the photosynthetic activity at single-cell level in *Haematococcus lacustris*

P.P. PATIL[*], K. NAGY[**], Á. ÁBRAHÁM[**,***], I. VASS[*,+], and M. SZABÓ[*,#,+]

Institute of Plant Biology, HUN-REN Biological Research Centre, 6726 Szeged, Hungary[*]
Institute of Biophysics, HUN-REN Biological Research Centre, 6726 Szeged, Hungary[**]
Doctoral School of Multidisciplinary Medical Sciences, University of Szeged, 6720 Szeged, Hungary[***]
Climate Change Cluster, University of Technology Sydney, Ultimo NSW 2007, Australia[#]

Abstract

Haematococcus lacustris is an important species of green algae because it produces the high-value carotenoid astaxanthin. Astaxanthin production is enhanced by various stress conditions causing the transformation of green vegetative cells to red cells with high amounts of astaxanthin, which plays various photoprotective and antioxidant roles. Although intensive research has been conducted to reveal the regulation of astaxanthin production, the photosynthetic capacity of the various cell forms is unresolved at the single-cell level. In this work, we characterized the photosynthetic and morphological changes of *Haematococcus* cells, using a combination of microfluidic tools and microscopic chlorophyll fluorescence imaging. We found marked but reversible changes in the variable chlorophyll fluorescence signatures upon the transformation of green cells to red cells, and we propose that the photosynthetic activity as revealed by single-cell chlorophyll fluorescence kinetics serves as a useful phenotypic marker of the different cell forms of *Haematococcus*.

Keywords: chlorophyll fluorescence; *Haematococcus lacustris*; photoprotection; photosynthesis; photosystem II.

Introduction

The green alga *Haematococcus lacustris* (hereafter denoted as *Haematococcus*) is capable of accumulating a massive amount of the valuable carotenoid astaxanthin (Ast). Ast has a high commercial value in the pharmaceutical, nutraceutical, and aquaculture industries (Boussiba 2000, Borowitzka 2013, Leu and Boussiba 2014). Therefore, this microalga has been the focus of intensive research efforts in the past decades. Particular focus has been directed towards the improvements of biomass and Ast yields which, however, requires the understanding of the physiology, cell cycle, and photosynthetic capacity of this species. As *Haematococcus* belongs to the carotenogenic algae, it undergoes a special life cycle and characteristic changes in cell morphology. *Haematococcus* can be transformed from motile, Ast-free vegetative green cells to Ast-rich immotile red haematocyst cells (Kobayashi *et al.* 1997), which involves several physiological and photosynthetic changes. Briefly, red cells acquire a significantly higher protective capacity against various stress factors than green cells; these include enhanced light screening

Highlights

- Single-cell level analysis of different cell forms of *Haematococcus lacustris*
- Altered chlorophyll fluorescence kinetics during green to red cell transformation
- Photosynthetic capacity is a single-cell phenotypic marker for astaxanthin production

Received 6 October 2023
Accepted 27 November 2023
Published online 18 December 2023

[+]Corresponding authors
e-mail: vass.imre@brc.hu
szabo.milan@brc.hu

Abbreviations: Ast – astaxanthin; Chl – chlorophyll; NPQ – nonphotochemical quenching; PAM – pulse amplitude modulation.
Acknowledgments: This work was supported by the National Research, Development, and Innovation Office (grant NKFIH FK 128977) and the grant GINOP-2.3.2-15-2016-00026. We thank Dr. Péter Galajda (BRC, Szeged) for fruitful discussions and for providing the microfluidic infrastructure.
Conflict of interest: The authors declare that they have no conflict of interest.

capacity, elevated antioxidant contents, scavenging of reactive oxygen species (ROS), and dissipation of excess light energy (reviewed in Solovchenko 2015).

The photosynthetic apparatus undergoes significant remodeling during cell transformation in *Haematococcus*. It has been shown that a transient upregulation in cell metabolism and energy-dependent photoprotective mechanisms occurs during the transformation of green cells to red cells to meet the energy demand of astaxanthin and fatty acid synthesis. However, in the more aged Ast-producing cells the nonphotochemical quenching (NPQ) declined (Chekanov *et al.* 2016, reviewed in Solovchenko *et al.* 2022) and the activity of PSII and PSI and cytochrome (cyt) b_6/f decreased (Tan *et al.* 1995), which was found to be associated with a minor fraction of Ast bound to the photosystems, leading to their destabilization (Mascia *et al.* 2017). These studies demonstrated the high potential and importance of chlorophyll (Chl) fluorescence analysis, which gives valuable information about light energy utilization, photochemical and nonphotochemical quenching, and the efficiency of PSII under various stress conditions (Schreiber 2004, Baker 2008, Kalaji *et al.* 2014), as well as the carotenogenic process in *Haematococcus* (Solovchenko *et al.* 2022). Other studies revealed the importance of alternative electron transfer processes, such as plastidial terminal oxidase (Scibilia *et al.* 2015), NAD(P)H dehydrogenase (NDH) (Patil *et al.* 2022a), and, in general, the activation of cyclic electron flow (Zhang *et al.* 2017) during cell transformation. Various aspects of the fast and slow fluorescence induction phenomena have been assessed, and it was found that the slow phase of the fluorescence transient, the so-called P-S-M-T phase is associated with transient activation of the energy-dependent q_E component of NPQ. In addition, after a saturation light pulse, the so-called low wave effect appeared, manifested by a transient drop of Chl fluorescence yield below the steady-state level, which effect was associated with the q_E component of NPQ (Fratamico *et al.* 2016). However, these mechanisms have not been investigated at the single-cell level and during the entire transformation process of green cells to red cells (and reversal of red to green cells).

The transformation of cells from the green to the red form, which impacts productivity and the yield of the valuable carotenoid astaxanthin, has been studied on macro and micro scales, involving microreactors (Kwak *et al.* 2015, Cheng *et al.* 2018). However, the physiological and morphological changes along with the Chl fluorescence characteristics on individually trapped cells over the time course of the carotenogenic process (and its reverse reaction) have not been monitored so far. We aimed to monitor simultaneously the morphological and photosynthetic activity changes at the single-cell level of *Haematococcus* by using the combination of microfluidics and variable Chl fluorescence imaging, which had been successfully applied on unicellular algae such as the widely used model organism *Chlamydomonas reinhardtii* (Széles *et al.* 2022, 2023) and the important coral symbiont *Symbiodinium* (Bashir *et al.* 2022). Chl fluorescence kinetics gives important information about the PSII–PSI intersystem electron transfer regulation. However, it remains unclear what the variability of the Chl fluorescence characteristics among individual cells is and how it changes over the cells' age, cell cycle, and during the transformation of vegetative cells to carotenogenic cells in *Haematococcus*. Therefore, the specific aims of this study were (*1*) to monitor the single-cell heterogeneity of frequently used Chl fluorescence parameters of PSII activity and (*2*) to record changes in fluorescence kinetics over time, during the Ast-producing phase.

Materials and methods

Culture conditions: *Haematococcus pluvialis* (strain code 358), recently referred to as *Haematococcus lacustris* (Girod-Chantrans) Roststafinski (Volvocales, Chlorophyceae) was obtained from the Culture Collection of Autotrophic Organisms (CCALA), Centre for Phycology, Institute of Botany of the AS CR, Třeboň, Czech Republic. For the experiments, it was grown in BG11 medium with 100 µmol(photon) m^{-2} s^{-1} white light illumination (12 h:12 h; day:night diurnal cycle), at a constant temperature of 24 ± 2°C, without shaking. For the microfluidic experiments, the cells were harvested in the early exponential phase (OD of 0.3 at 720 nm).

Microfluidic setup: The microfluidic chamber was fabricated from PDMS (polydimethylsiloxane) and bound on the cover slip. According to the cell size, an array of U-shaped traps was created in the chamber with the dimensions of 40-µm width and 50-µm length; the traps had 10-µm wall thickness with 5-µm gap; the chamber had inlet and outlet holes (Bashir *et al.* 2022).

The cells were loaded with a pipette through the inlet hole (it was made sure that each trap had 1–2 cells). One end of a long tube was attached to the inlet hole and the other end of the tube was connected to the 1-mL syringe (*Omnifix-F Solo Luer* 1 mL, *B. Braun*) containing the media to flow through the microfluidic device throughout the experiment. The syringe was mounted onto the pump (*SyringeTwo-SKU 4000*, *New Era Pump Systems*, *Inc.*, USA) with the flow rate set to 20 µL h^{-1}. A small tube was placed in the outlet hole of the chamber; the other end of the tube was kept open for the flow of media to pass through. The microfluidic chamber was mounted in an inverted position on the microscope platform.

The cells were observed with a 25× objective lens (*Hund Wetzlar*, *Helmut Hund GmbH*, Wetzlar, Germany) in the light microscope (*H 600/12*, *Hund Wetzlar*, *Helmut Hund GmbH*, Wetzlar, Germany). The microscope was equipped with a *MicroQ* digital camera (*UCMOS08000KPB*, *ToupTek Photonics Co.*, *Ltd*., Hangzhou, China). Single-cell photophysiology was assessed by variable Chl fluorescence measurements using a microscopy version of a PAM Chl fluorescence imaging system (*Imaging-PAM M-Series* Chlorophyll Fluorometer, microscopy version, *Heinz Walz GmbH*, Effeltrich, Germany). The morphology of the cells was constantly captured through images every 60 s with a camera control software named *ToupView* (*ToupTek Photonics Co.*, *Ltd*., Hangzhou, China) (Bashir *et al.* 2022).

Experimental procedure: The cells in the microfluidic chamber were illuminated with 100 µmol(photon) m^{-2} s^{-1} (10 h:14 h; day:night diurnal cycle). The day and night cycle was adjusted manually by changing the light filters (blue-white filter for day and green filter for night), the aperture focus (set to higher in the day and lower during the night), and the light intensity [100 µmol(photon) m^{-2} s^{-1} during the day and 0.1 µmol(photon) m^{-2} s^{-1} during the night]. After 48 h from the initiation of the experiment, the medium in the syringe was changed from normal BG11 to nitrate-free BG11 medium containing 50 mM sodium acetate (for the transformation of green cells to red cells, *see e.g.*, Kakizono *et al.* 1992). The cells were incubated in this medium for 7 d until they completely turned into red cysts. For the cells to re-green, the medium in the chamber provided through the syringe was replaced with normal BG11 medium on the 7th day. The photophysiology and morphology data of the cells were recorded until the 15th day.

Single-cell chlorophyll fluorescence measurements (microscopy imaging PAM analysis): Single-cell photophysiological Chl fluorescence parameters, such as PSII activity, slow induction and recovery curves, and rapid light curves were determined by pulse-amplitude modulated imaging (PAM) microfluorometry (*Imaging-PAM M-Series* chlorophyll fluorometer, microscopy version, with an *IMAG-CG* control unit and *IMAG-L450* measuring head, *Heinz Walz GmbH*, Effeltrich, Germany) which was equipped with an *IMAG-K6* CCD camera (*Allied Vision Technologies GmbH*, Ahrensburg, Germany). To avoid artifacts during the measurement (baseline correction before the measurement) of the biological sample in the high sensitivity mode (which is required to obtain variable fluorescence image of cells with appropriate S/N), a non-biological fluorescence standard was used to equalize the maximum fluorescence yield (F_m) to minimum fluorescence yield (F_0). Once the steady-state fluorescence yield (F_0) stabilized, an F_0 image was obtained [measuring light intensity = 4, approx. 0.3 µmol(photon) m^{-2} s^{-1}, gain = 10, frequency = 1, damping = 1, F_0 averaging n = 3] after 3 min of dark adaptation. A saturating pulse of blue light [470 nm, approx. 2,000 µmol(photon) m^{-2} s^{-1}, 0.8-s pulse width] was applied to obtain F_m images, and the F_v/F_m parameter, which reflects PSII activity, was calculated as $F_v/F_m = (F_m - F_0)/F_m$.

A slow induction measuring protocol was initiated after 3 min of the dark adaptation [measuring light intensity = 4, approx. 0.3 µmol(photon) m^{-2} s^{-1}, gain = 10, damping = 1, actinic light intensity = 5 = 114 µmol(photon) m^{-2} s^{-1}]. After the start of Chl fluorescence recording, the first saturation pulse was given in the dark at 10 s and the Chl fluorescence signals were recorded for 40 s in the dark to establish a baseline. Then the actinic light (wavelength of approx. 470 nm) at ~114 µmol(photon) m^{-2} s^{-1} (or near the growth light intensity) was switched on to record light-induced Chl fluorescence change for approx. 230 s. At 200 s, a second saturating pulse was given (during the actinic light), and subsequently, the Chl fluorescence change from light to dark was monitored up to 400 s, similarly at 300 s, a saturating pulse (3rd pulse) was applied during the dark measurement.

The photosynthesis *vs*. irradiance curves (rapid light curves) were recorded using an automated protocol that applied progressively increasing actinic irradiance steps up to 400 µmol(photon) m^{-2} s^{-1}. The length of the individual light steps was 20 s. Nonphotochemical quenching (NPQ) was calculated as $NPQ = (F_m - F_m')/F_m$, where F_m and F_m' are the maximal fluorescence yields in the dark-adapted state and during actinic illumination, respectively.

Inhibitor treatments: Nigericin treatment was performed in the same microfluidic setup as described above. After loading the green cells of *Haematococcus*, the first microscopy PAM measurements were done after 18 h of incubation with BG11 to recover from loading stress. Then the syringe was replaced with another containing a new solution containing BG11 + 1 µM nigericin. Since the effect of nigericin was not complete even after a 29-h treatment, a new solution was added and the nigericin concentration was raised to 3 µM. After a 16-h treatment with 3 µM nigericin, the PAM measurements were done again. During the entire experiment, the same trapped cells were monitored and measured. The flow rate was set to 20 µL h^{-1} throughout. The time course of the flow of the solution from the syringe to the microfluidic traps was verified using a red-colored food dye, using the same experimental conditions as for physiological assays of *Haematococcus* cells.

Results

We monitored the changes in Chl fluorescence and photosynthetic activity in cells that were trapped in microfluidic chambers. This system allowed the monitoring of the time-dependent changes in physiological and morphological parameters with high resolution, under precisely adjusted environmental conditions at a constant flow and minimal turbulence/shearing effect.

Haematococcus cells in the green vegetative stage were loaded into the microfluidic chambers (Fig. 1*A*, microscopic images). PSII efficiency (F_v/F_m) of the individual cells was in the range of 0.61–0.69 (Fig. 1*B*, PAM Chl fluorescence image). The analysis of the transient changes in Chl fluorescence kinetics revealed condition-specific features. The first saturation pulse in the dark was followed by a dip, also called the low wave phenomenon in the fluorescence yield, which was also visible after the 3rd saturation pulse (in darkness). The fluorescence dip also existed during the actinic illumination (2nd saturation pulse) (Fig. 1*C* – typical signal of a single green cell, Fig. 1*D* – average ± SD of normalized Chl fluorescence traces, the first time point was set to 0 to display relative fluorescence changes).

Acetate treatment in combination with nitrate-free BG11 caused the transformation of green cells to red cells (Fig. 1*E*), which resulted in a drastic decrease in the Chl fluorescence signal (Fig. 1*F*,*G*). Although certain red cells maintained F_v/F_m of about 0.65–0.68, the large decrease

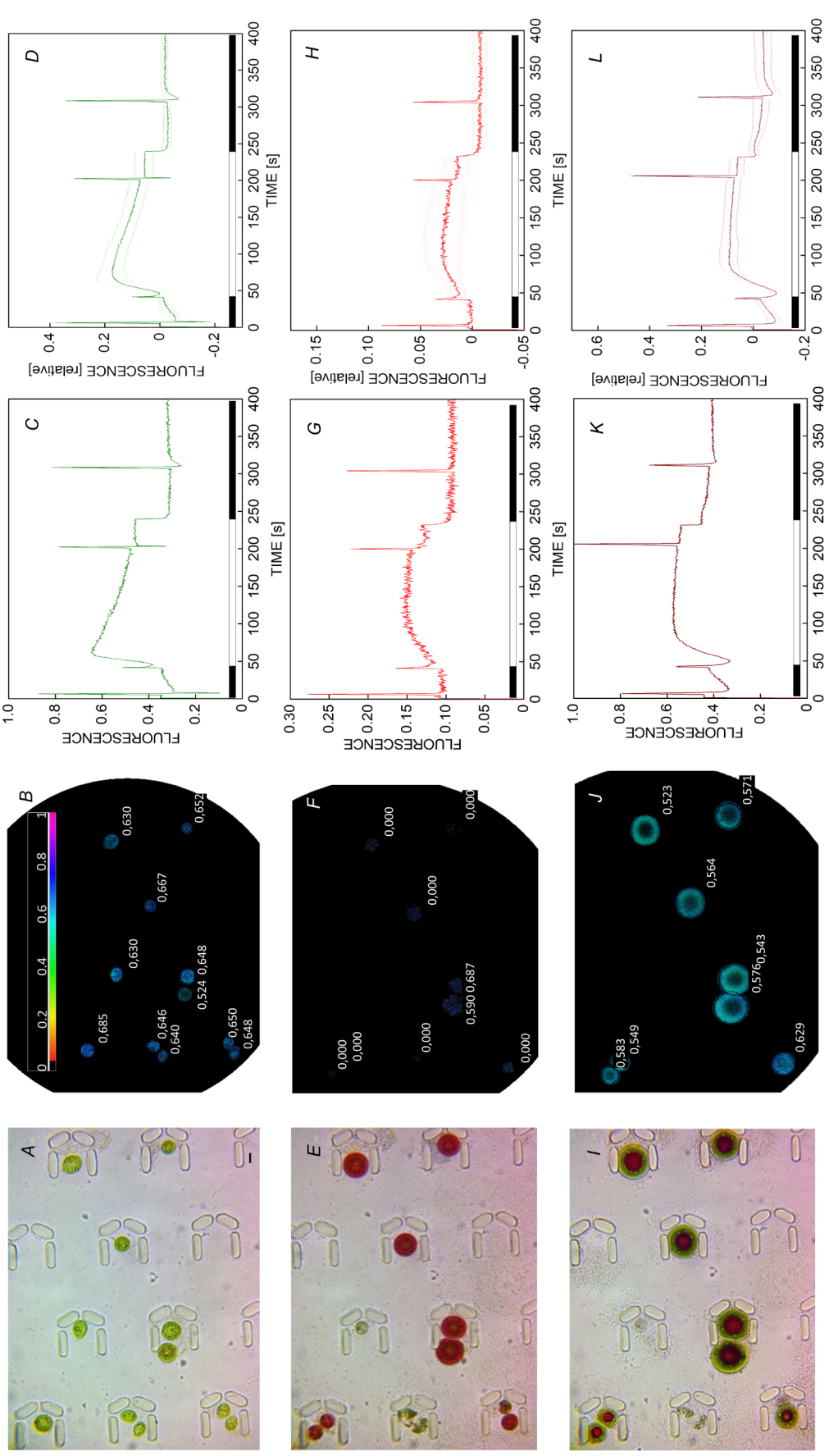

Fig. 1. *Haematococcus* green cells (*A–D*), red cells (*E–H*), and cells transformed back from red to green stage (*I–L*) trapped in microfluidic chambers; light microscopy images (*A,E,I*), variable Chl fluorescence images of PSII efficiency (F_v/F_m) (*B,F,J*), representative original Chl fluorescence kinetics of the individual cells (*C,G,K*), normalized Chl fluorescence kinetics (initial fluorescence adjusted to 0 to represent relative changes, average ± SD, $n = 8$) (*D,H,L*). *Closed black bars* above the X scale represent the dark periods, and the *open white bar* represents the actinic light illumination period. Scale bar (*A*) represents 10 μm.

in the Chl fluorescence signal made precise determination of the F_v/F_m of single red cells difficult. Nevertheless, the fluorescence kinetic traces could be properly recorded (Fig. 1*G*), and the cells displayed variable fluorescence (although with a marked decrease in the overall fluorescence intensity, *cf.* Fig. 1*C* and 1*G*). Therefore, the red cells remained photosynthetically competent despite the large decrease in the Chl fluorescence signal. More importantly, the fluorescence kinetics underwent remarkable changes in red cells, with the most apparent observation that the fluorescence dips following saturation pulses given in the dark, *i.e.*, in the absence of actinic light, could not be observed. During the actinic light period, the cells displayed a small dip in fluorescence intensity after a saturation pulse, but the recovery of fluorescence (the increase in fluorescence after the dip) was much slower than that in the green cells (Fig. 1*G*,*H*).

After the re-establishment of control conditions (full BG11 without acetate), the red cells partially regained the green vegetative stage, although significant Ast remained in the cells until the end of the experiment. The size of the cells also remained larger than that of the control green cells (Fig. 1*I*). Cells also regained the variable Chl fluorescence signal, although the F_v/F_m values of re-greened cells were lower than those of the green stage at the beginning of the experiment (Fig. 1*J*). This decline in F_v/F_m also occurred when the cells were kept in the green stage in BG11 for the same period as in the case of the Ast-producing experiment (Fig. 1S, *supplement*), indicating that towards the end of the experiment, the PSII activity of trapped *Haematococcus* tends to decline. In the fluorescence kinetics of the re-greened cells, the dip after saturation pulse in the dark phases (before and after actinic illumination) reappeared but, interestingly, during actinic light the fluorescence dips after saturation pulses did not recover (Fig. 1*K*,*L*).

Comparison of the fluorescence kinetic changes of the different cell stages shows that green cells displayed a dip, or low wave, in the fluorescence after a saturation pulse, given either during the actinic illumination or in the dark (Fig. 2*A*). In contrast, in the red cells, the fluorescence dip was missing after the saturation pulse (Fig. 2*B*), which could be partially regained when the cells were incubated again in BG11 (Fig. 2*C*).

Fluorescence kinetics were also recorded in cells that were kept in the green stage for the entire experiment (in BG11 without acetate treatment). Although some alterations of the fluorescence kinetics profiles occurred and the fluorescence profiles became more heterogeneous towards the end of the experiment, the cells maintained the 'low wave' feature when they were maintained in the green stage for the entire time (Fig. 3), indicating also that the cells remained in the green stage without Ast production.

The photosynthesis *vs*. irradiance curves (rapid light curves) also revealed characteristic changes in the nonphotochemical quenching (NPQ). In green cells at the beginning (day 1) and also after the regeneration from

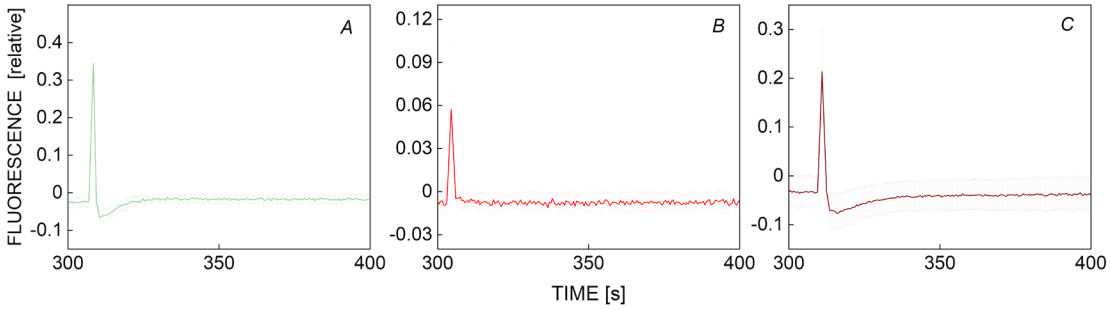

Fig. 2. Fluorescence kinetics after a saturation pulse (3rd saturation pulse in the second dark phase) in the different cell types of *Haematococcus*. *A* – green cells (day 1), *B* – red cells (day 8), *C* – regenerated green cells (day 13).

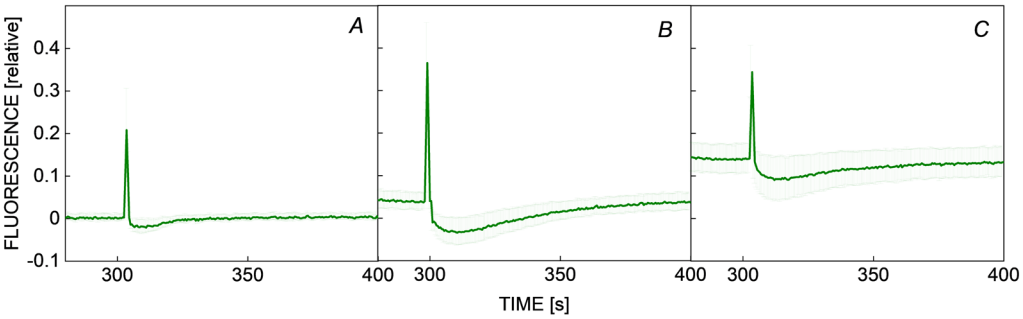

Fig. 3. Fluorescence kinetics after a saturation pulse (3rd saturation pulse in the second dark phase) in green cells of *Haematococcus*, which were kept in the green stage during the entire experiment. *A*, *B*, and *C* indicate the same time points as the experiment in Fig. 2, *i.e.*, days 1, 8, and 13, respectively.

red to green cells (day 13), the NPQ exhibited a transient increase followed by a decrease and a slight increase at progressively increasing irradiances. In contrast, red cells (day 8) exhibited a progressively increasing NPQ with increasing irradiance and lacked the initial transient NPQ at lower irradiances (Fig. 4). Cells after re-greening displayed similar NPQ characteristics as the initial green cells, but the transient increase in NPQ at lower irradiances was larger (day 13) as compared to NPQ in green cells at the beginning of the experiment (day 1).

When the cells were kept in the green state for the same period as in the green-to-red-re-green transition experiments, the transient NPQ increase was present for the entire duration of the experiment, although the characteristics of NPQ kinetics changed showing the maximal NPQ level at higher light intensities with increasing time (Fig. 5).

To investigate whether the condition-specific Chl fluorescence signal displays heterogeneity in various cells at the same measuring time point, the photosynthetic

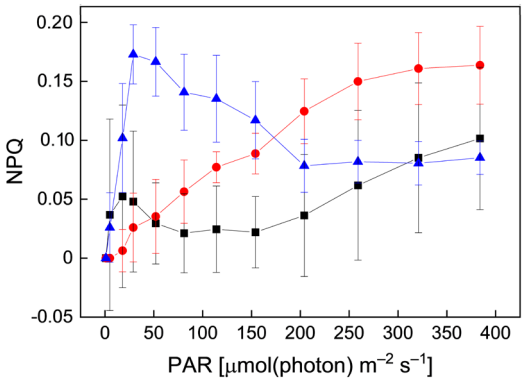

Fig. 4. Nonphotochemical quenching (NPQ) as a function of irradiance (rapid light curve) in the different cell types. Green cells (day 1, *black squares*), red cells (day 8, *red circles*), and re-greened cells (day 13, *blue triangles*).

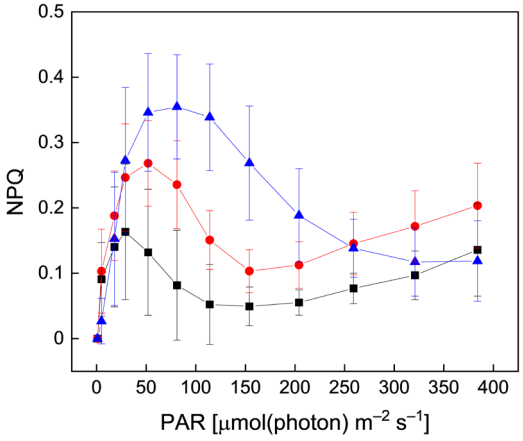

Fig. 5. Nonphotochemical quenching (NPQ) as a function of irradiance (rapid light curve) in cells that were retained in the green stage for the entire experiment. Green cells on day 1 (*black squares*), day 8 (*red circles*), and day 13 (*blue triangles*).

properties were analyzed in the experimental period when the cell culture just entered the transition phase from green to red cells. The cells in the transition phase, after one day of acetate treatment, showed an onset of accumulation of Ast, indicated by the appearance of red globules towards the center of the cells (Fig. 6*A*). The F_v/F_m of the cells remained mostly in the range of 0.61–0.68 (Fig. 6*B*). However, the cells displayed considerable heterogeneity in fluorescence kinetics (Fig. 6*C*) and NPQ trajectory (Fig. 6*D*), which attests to the mixed characteristics of green and red cells. This observation indicates that *Haematococcus* cells in the transition phase from green to red stage display a more heterogeneous photosynthetic response than do the cells that are in stationary condition (either in green or deep red stage).

Discussion

In this study, the morphological features of the industrially important green alga *Haematococcus* were characterized along with their photosynthetic capacity in microfluidic chambers. This approach has significant advantages as compared to bulk measurements, because in suspensions the cell-to-cell variability of photosynthetic performance, and the relationship between the photosynthetic capacity and morphology cannot be revealed. In microalgae that have high applied relevance, morphological analysis along with photosynthetic capacity is particularly important, because the value of the organism is determined by the information available about its light-energy utilization and its timescale of producing valuable compounds.

The current study revealed single-cell variability of the commonly used parameter, F_v/F_m, which, although frequently used, has been under intensive investigation recently, and it is now denoted as PSII efficiency rather than the previously preferred terminology of PSII quantum yield (Sipka *et al.* 2021). More strikingly, Chl fluorescence kinetics occurring after saturation pulses or dark-to-light transitions revealed specific features. The so-called low wave fluorescence transient is manifested by a brief reversible lowering (dip) of Chl fluorescence yield after saturating multi-turnover pulses given either in the dark-adapted state or during actinic illumination (Larcher and Neuner 1989, Xyländer and Hagen 2002, Tsuyama *et al.* 2004, Fratamico *et al.* 2016). Such low waves were observed in *Haematococcus* and were suggested to arise either from transiently increased nonphotochemical quenching, as a result of the formation of a trans-thylakoid proton gradient due to cyclic electron flow around PSI (Fratamico *et al.* 2016), or from an imbalance between the charge separation capacity of the photosystems and the electron buffering capacity of the intersystem electron transport pool (Hagen *et al.* 1992).

Another specific fluorescence transient is the so-called post-illumination fluorescence rise, which is manifested as a transient decrease of the fluorescence yield after switching off the actinic light followed by its recovery in the dark (Shikanai *et al.* 1998). This effect is related to the backflow of electrons from stromal electron carriers to the PQ pool in the dark, but not related to NPQ phenomena

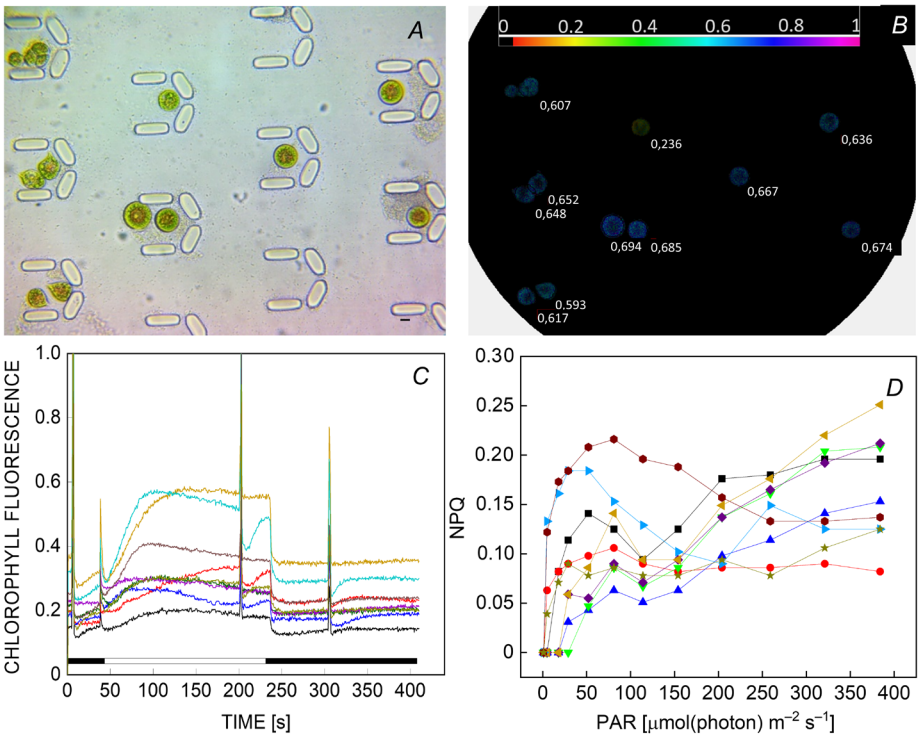

Fig. 6. Morphological and photosynthetic changes in *Haematococcus* cells after 1 d of acetate treatment. This state represents the transition stage (or intermediate stage) from green to red cells. Light microscopy images (*A*), variable Chl fluorescence images of PSII efficiency (F_v/F_m) (*B*), representative original Chl fluorescence kinetics of the individual cells (*C*), and nonphotochemical quenching (NPQ) based on the light curve measurements (*D*). The fluorescence kinetics and NPQ curves are not averaged to show the cell-to-cell variability. *Closed black bars* above the X scale represent the dark periods, and the *open white bar* represents the actinic light illumination period. Scale bar (*A*) represents 10 µm.

(Munekage *et al.* 2004), and reflects the NDH-induced reduction of the PQ pool in the dark (Yamori *et al.* 2015). A related fluorescence wave phenomenon also occurs after single turnover flash illumination in cyanobacteria (Deák *et al.* 2014) and various microalgae (Krishna *et al.* 2019, Mohammad Aslam *et al.* 2022, Patil *et al.* 2022a,b) under anaerobic conditions, which arises from transient oxidation of the PQ pool due to more efficient electron extraction by PSI than electron inflow from PSII, followed by re-reduction of the PQ pool from stromal components *via* the NDH1 (cyanobacteria) or NDH2 complexes (green algae). However, this phenomenon could not be observed in the green cells of *Haematococcus*; it could be induced only in the red cells under the combination of anaerobic conditions and inhibited PSII activity (Patil *et al.* 2022a).

Under our conditions, the post-illumination fluorescence rise phenomenon could not be observed either in the green or in the red cells, although it was reported in a previous study in partly desiccated *Haematococcus* cells (Roach *et al.* 2022), and we could also observe it in bulk cultures (not shown). The lack of the post-illumination fluorescence rise under our conditions is consistent with the lack of the related single turnover flash-induced fluorescence wave (Patil *et al.* 2022a) and may be related to illumination conditions, especially to the blue actinic light used by the microscopy setup *vs*. the red actinic illumination typically used in measurements using bulk cultures.

Although the post-illumination fluorescence rise could not be unequivocally identified at single-cell level, the low-wave phenomenon was visible in individual green cells after a saturation pulse in the dark following the actinic illumination [in agreement with previous studies obtained in bulk cultures (Larcher and Neuner 1989, Xyländer and Hagen 2002, Tsuyama *et al.* 2004, Fratamico *et al.* 2016)], but not in red cells (Figs. 1, 2). In contrast to the post-illumination fluorescence rise, which is related to NDH-mediated reduction of the PQ pool (Munekage *et al.* 2004, Yamori *et al.* 2015), the low wave phenomenon is assigned to transient NPQ due to trans-thylakoid proton gradient formation *via* cyclic electron flow around PSI (Fratamico *et al.* 2016). Therefore, we checked the effect of nigericin that eliminates the proton gradient.

Our data show that in green cells nigericin prevents the formation of the low wave (Fig. 7*B*) and prevents the formation of transient NPQ (Fig. 7*C*). The long timecourse of the nigericin effect in the microfluidic traps is due to the time required for the nigericin solution to reach the cells trapped in the chamber, which was estimated to take about 6 h. Nevertheless, it could be clearly shown that nigericin largely eliminated the low wave, along with the transient NPQ, in agreement with Fratamico *et al.* (2016). Furthermore, similar results concerning the inhibitory effect of nigericin were obtained

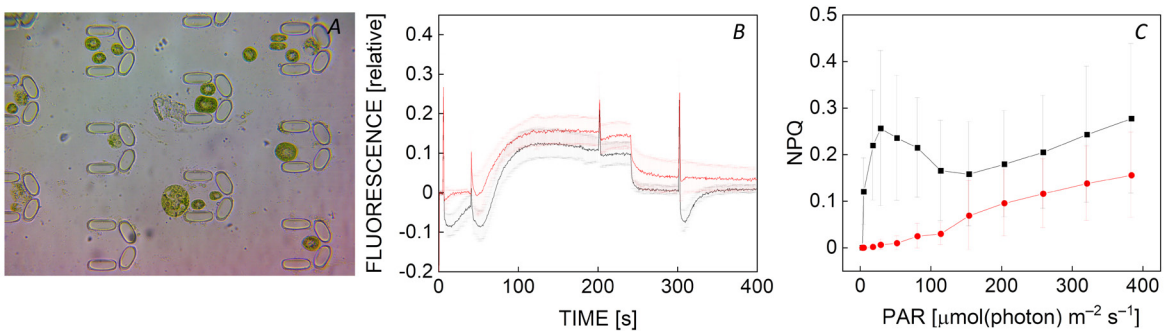

Fig. 7. Effect of nigericin on the Chl fluorescence kinetics (*B*) and NPQ (*C*) of green *Haematococcus* cells (*A*). *Black line* – control, no treatment; *red line* – nigericin treatment (3 μM for 16 h). Average ± SD (n = 8).

in bulk cultures (not shown), confirming its assignment to trans-thylakoid proton gradient formation. The lack of the low wave fluorescence transient in the red cells may be due to their acclimation state and the enhanced photoprotective capacity of astaxanthin, which did not require the transient build-up of NPQ in red cells.

NPQ is an important protective mechanism against high light stress since it ensures the dissipation of excess light energy that could damage the photosynthetic apparatus. The trajectory and NPQ characteristics as a function of irradiance were markedly different in the case of single green and red cells. Green cells responded with a rapid transient increase of NPQ with increasing light intensities followed by stabilization at a lower equilibrium level. In contrast, in the red cells, NPQ increased progressively with increasing irradiances (Fig. 4) providing high sustained NPQ at high light, in agreement with previous findings which showed that at the onset of high light stress, NPQ increased and the elevated level of NPQ became nearly constant (Chekanov *et al.* 2016). The response may be due to the presence of protective Ast, which can provide sufficient photoprotection at lower light intensities without the need for an NPQ response at low light intensities. In the recovery stage from red to green cells, the NPQ *vs*. irradiance curve regained the characteristics of initial green cells, *i.e.*, the transient activation of NPQ at lower irradiances followed by a decrease with progressively increasing irradiance (although the overall NPQ was higher in the recovered green cells than in the initial green cells). A plausible explanation for a transient rise of NPQ in green vegetative cells (and after regeneration from the red Ast-producing stage) is a capability for rapid adjustment that protects the green cells from light fluctuations, and therefore it prevents wasteful light energy dissipation when the conditions are favorable (Chekanov *et al.* 2016).

It has to be noted that the NPQ measured here is based on rapid light curves, which could be obtained in a short time with minimal possible disturbance of cells during the prolonged measurements (*i.e.*, the continuous observation of cells in microfluidic chambers). Although rapid light curves do not give information about photosynthetic activity, in steady-state conditions they could provide information about the photosynthetic flexibility and activation of NPQ in response to rapid changes in irradiance (Ralph and Gademann 2005, Brestic and Zivcak 2013, Kalaji *et al.* 2014), and help distinguish the photoprotective responses of single green or red cells. While the transient nature of the NPQ increase requires further investigation, it is clear from the present study that the different cell forms of *Haematococcus* can be suitably discerned based on their Chl fluorescence signals and therefore specific information could be gained about condition-specific features based on Chl fluorescence kinetics at single-cell level.

It is an important finding in our work that when the *Haematococcus* cells are either in the green or red stage, their Chl fluorescence properties are quite homogeneous, and the two cell types can be clearly distinguished based on their single-cell photosynthetic response. This was verified by the control experiment in which cells were maintained in the green stage for the entire time of the experiment; under these conditions, *Haematococcus* cells maintained the 'low wave' fluorescence profile (Fig. 3), in contrast to red cells, which did not display this feature. Whether *Haematococcus* cells experience any limitation or the cell cycle may be perturbed in microfluidic conditions requires further investigations. Nonetheless, the alteration of the fluorescence kinetic profile with the large decrease in fluorescence intensity and the loss of the 'low wave' feature is a specific trait of Ast-producing red cells and not caused by any perturbation in the experimental conditions.

It is an important question in the field of single-cell analysis whether cell-specific traits, cell-to-cell variability, and Chl fluorescence heterogeneity can be revealed, which are not possible to identify in macroscopic bulk samples. To investigate this possibility, cells in the transition from the green to the red stage (*i.e.*, shortly after the induction of Ast production) were analyzed (Fig. 6). While no morphological changes or significant alterations of the basic PSII activity parameter F_v/F_m could be observed, the fluorescence kinetics and the trajectory of NPQ indicated marked heterogeneity. This highlights the advantage of the time-dependent analysis of cell morphology in combination with photosynthetic responses at a single-cell level, because even though morphological features remain similar in a cell population, during transiently changing

physiological conditions, the underlying photosynthetic activity could display significant cell-to-cell variability.

In conclusion, the method presented here is based on cell-type specific Chl fluorescence signatures. The main advantage of single-cell Chl fluorescence analysis as performed here was to reveal the subtle heterogeneity of individual cells at different physiological states of carotenogenic microalgae, which would remain undetected in bulk measurements. Furthermore, the low wave phenomenon in Chl fluorescence in conjunction with the analysis of transiently activated NPQ allowed the assignment of cell type-specific photosynthetic properties. This is particularly valuable when the metabolic state of carotenogenic algae changes, for example at the induction of astaxanthin production or the reversal of carotenogenic cells to vegetative cells. Therefore, this approach has a useful potential to monitor the Ast-producing process and the timescale of various stress factors or treatments that may accelerate the production of this highly valuable carotenoid.

References

Baker N.R.: Chlorophyll fluorescence: A probe of photosynthesis *in vivo*. – Annu. Rev. Plant Biol. **59**: 89-113, 2008.

Bashir F., Kovács S., Ábrahám Á. *et al.*: Viable protoplast formation of the coral endosymbiont alga *Symbiodinium* spp. in a microfluidics platform. – Lab Chip **22**: 2986-2999, 2022.

Borowitzka M.A.: High-value products from microalgae – their development and commercialisation. – J. Appl. Phycol. **25**: 743-756, 2013.

Boussiba S.: Carotenogenesis in the green alga *Haematococcus pluvialis*: Cellular physiology and stress response. – Physiol. Plantarum **108**: 111-117, 2000.

Brestic M., Zivcak M.: PSII fluorescence techniques for measurement of drought and high temperature stress signal in crop plants: protocols and applications. – In: Rout G.R., Das A.B. (ed.): Molecular Stress Physiology of Plants. Pp. 87-131. Springer, India 2013.

Chekanov K., Lukyanov A., Boussiba S. *et al.*: Modulation of photosynthetic activity and photoprotection in *Haematococcus pluvialis* cells during their conversion into haematocysts and back. – Photosynth. Res. **128**: 313-323, 2016.

Cheng X., Qi Z., Burdyny T. *et al.*: Low pressure supercritical CO_2 extraction of astaxanthin from *Haematococcus pluvialis* demonstrated on a microfluidic chip. – Bioresource Technol. **250**: 481-485, 2018.

Deák Z., Sass L., Kiss É. *et al.*, Vass I.: Characterization of wave phenomena in the relaxation of flash-induced chlorophyll fluorescence yield in cyanobacteria. – BBA-Bioenergetics **1837**: 1522-1532, 2014.

Fratamico A., Tocquin P., Franck F.: The chlorophyll *a* fluorescence induction curve in the green microalga *Haematococcus pluvialis*: further insight into the nature of the P–S–M fluctuation and its relationship with the "low-wave" phenomenon at steady-state. – Photosynth. Res. **128**: 271-285, 2016.

Hagen C., Bornman J.F., Braune W.: Reversible lowering of modulated chlorophyll fluorescence after saturating flashes in *Haematococcus lacustris* (Volvocales) at room temperature. – Physiol. Plantarum **86**: 593-599, 1992.

Kakizono T., Kobayashi M., Nagai S.: Effect of carbon/nitrogen ratio on encystment accompanied with astaxanthin formation in a green alga, *Haematococcus pluvialis*. – J. Ferment. Bioeng. **74**: 403-405, 1992.

Kalaji H.M., Schansker G., Ladle R.J. *et al.*: Frequently asked questions about *in vivo* chlorophyll fluorescence: practical issues. – Photosynth. Res. **122**: 121-158, 2014.

Kobayashi M., Kurimura Y., Kakizono T. *et al.*: Morphological changes in the life cycle of the green alga *Haematococcus pluvialis*. – J. Ferment. Bioeng. **84**: 94-97, 1997.

Krishna P.S., Morello G., Mamedov F.: Characterization of the transient fluorescence wave phenomenon that occurs during H_2 production in *Chlamydomonas reinhardtii*. – J. Exp. Bot. **70**: 6321-6336, 2019.

Kwak H.S., Kim J.Y.H., Sim S.J.: A microreactor system for cultivation of *Haematococcus pluvialis* and astaxanthin production. – J. Nanosci. Nanotechnol. **15**: 1618-1623, 2015.

Larcher W., Neuner G.: Cold-induced sudden reversible lowering of *in vivo* chlorophyll fluorescence after saturating light pulses: A sensitive marker for chilling susceptibility. – Plant Physiol. **89**: 740-742, 1989.

Leu S., Boussiba S.: Advances in the production of high-value products by microalgae. – Ind. Biotechnol. **10**: 169-183, 2014.

Mascia F., Girolomoni L., Alcocer M.J.P. *et al.*: Functional analysis of photosynthetic pigment binding complexes in the green alga *Haematococcus pluvialis* reveals distribution of astaxanthin in Photosystems. – Sci. Rep.-UK **7**: 16319, 2017.

Mohammad Aslam S., Patil P.P., Vass I., Szabó M.: Heat-induced photosynthetic responses of Symbiodiniaceae revealed by flash-induced fluorescence relaxation kinetics. – Front. Mar. Sci. **9**: 932355, 2022.

Munekage Y., Hashimoto M., Miyake C. *et al.*: Cyclic electron flow around photosystem I is essential for photosynthesis. – Nature **429**: 579-582, 2004.

Patil P.P., Mohammad Aslam S., Vass I., Szabó M.: Characterization of the wave phenomenon of flash-induced chlorophyll fluorescence in *Chlamydomonas reinhardtii*. – Photosynth. Res. **152**: 235-244, 2022b.

Patil P.P., Vass I., Szabó M.: Characterization of the wave phenomenon in flash-induced fluorescence relaxation and its application to study cyclic electron pathways in microalgae. – Int. J. Mol. Sci. **23**: 4927, 2022a.

Ralph P.J., Gademann R.: Rapid light curves: A powerful tool to assess photosynthetic activity. – Aquat. Bot. **82**: 222-237, 2005.

Roach T., Fambri A., Ballesteros D.: Humidity and light modulate oxygen-induced viability loss in dehydrated *Haematococcus lacustris* cells. – Oxygen **2**: 503-517, 2022.

Schreiber U.: Pulse-amplitude-modulation (PAM) fluorometry and saturation pulse method: An overview. – In: Papageorgiou G.C., Govindjee (ed.): Chlorophyll *a* Fluorescence: A Signature of Photosynthesis. Pp. 279-319. Springer, Dordrecht 2004.

Scibilia L., Girolomoni L., Berteotti S. *et al.*: Photosynthetic response to nitrogen starvation and high light in *Haematococcus pluvialis*. – Algal Res. **12**: 170-181, 2015.

Shikanai T., Endo T., Hashimoto T. *et al.*: Directed disruption of the tobacco *ndhB* gene impairs cyclic electron flow around photosystem I. – PNAS **95**: 9705-9709, 1998.

Sipka G., Magyar M., Mezzetti A. *et al.*: Light-adapted charge-separated state of photosystem II: structural and functional dynamics of the closed reaction center. – Plant Cell **33**: 1286-1302, 2021.

Solovchenko A., Lukyanov A., Vasilieva S., Lobakova E.: Chlorophyll fluorescence as a valuable multitool for microalgal biotechnology. – Biophys. Rev. **14**: 973-983, 2022.

Solovchenko A.E.: Recent breakthroughs in the biology of astaxanthin accumulation by microalgal cell. – Photosynth.

Res. **125**: 437-449, 2015.
Széles E., Kuntam S., Vidal-Meireles A. *et al.*: Single-cell microfluidics in combination with chlorophyll *a* fluorescence measurements to assess the lifetime of the *Chlamydomonas* PSBO protein. – Photosynthetica **61**: 417-424, 2023.
Széles E., Nagy K., Ábrahám Á. *et al.*: Microfluidic platforms designed for morphological and photosynthetic investigations of *Chlamydomonas reinhardtii* on a single-cell level. – Cells **11**: 285, 2022.
Tan S., Cunningham Jr. F.X., Youmans M. *et al.*: Cytochrome *f* loss in astaxanthin-accumulating red cells of *Haematococcus pluvialis* (Chlorophyceae): comparison of photosynthetic activity, photosynthetic enzymes, and thylakoid membrane polypeptides in red and green cells. – J. Phycol. **31**: 897-905, 1995.
Tsuyama M., Shibata M., Kawazu T., Kobayashi Y.: An analysis of the mechanism of the low-wave phenomenon of chlorophyll fluorescence. – Photosynth. Res. **81**: 67-76, 2004.
Xyländer M., Hagen C.: 'Low-waves' in chlorophyll fluorescence kinetics indicate deprivation of bicarbonate. – Photosynth. Res. **72**: 255-262, 2002.
Yamori W., Shikanai T., Makino A.: Photosystem I cyclic electron flow via chloroplast NADH dehydrogenase-like complex performs a physiological role for photosynthesis at low light. – Sci. Rep.-UK **5**: 13908, 2015.
Zhang L., Su F., Zhang C. *et al.*: Changes of photosynthetic behaviors and photoprotection during cell transformation and astaxanthin accumulation in *Haematococcus pluvialis* grown outdoors in tubular photobioreactors. – Int. J. Mol. Sci. **18**: 33, 2017.